J Mar Sci Technol (2011) 16:214–225
DOI 10.1007/s00773-010-0113-y

ORIGINAL ARTICLE

Theory of a subjective vertical–horizontal conflict physiological motion sickness model for contemporary ships

Hassan Khalid · Osman Turan · Jelte E. Bos

Received: 7 March 2010 / Accepted: 7 November 2010 / Published online: 20 January 2011

Abstract Subjective vertical (SV) conflict theory postulates that motion sickness is elicited in all situations that lead to a difference between the sensed and subjective verticals. The sensed vertical is Earth's gravity as perceived by human sense modalities; the subjective vertical is also Earth's gravity, but in accordance with the expectations of the central nervous system, based on past interaction with the spatial environment. The SV conflict models have been successfully used to predict motion sickness on board high speed passenger ferries. However, a recent EU project, COMPASS, indicated that the role of horizontal accelerations in the elicitation of motion sickness aboard contemporary vessels is as important as that of vertical accelerations. Consequently, this paper, using an extended statement of the SV conflict theory, proposes that SV conflict models can be further elaborated by explicitly incorporating the effects of horizontal accelerations (normal to gravity) experienced aboard contemporary vessels. It is hypothesized that the explanation of motion sickness variability can be improved by considering the combined effects of subjective vertical conflict and subjective horizontal conflict (the difference between the sensed and expected horizontal accelerations). After presenting the theoretical aspects of subjective vertical–horizontal (SVH) conflict model, this paper demonstrates its application to 7 field trials of 3 different vessels. The proportion of commuters getting seasick (i.e., motion sickness incidences, MSI) during each field trial, has been statistically compared with the values predicted by the physiological (SVH and SV) and descriptive sickness prediction models. In general, SVH conflict model is outperforming the descriptive models and displaying approximately 20% improvement over the SV conflict model.

Keywords Motion sickness · Subjective vertical · Subjective vertical horizontal · Sensory conflict · Vestibular system · Physiological motion sickness model

H. Khalid (✉) · O. Turan
Marine Design, Operation and Human Factors,
Department of Naval Architecture and Marine Engineering,
University of Strathclyde, 100 Montrose Street,
Glasgow G4 0LZ, Scotland, UK
e-mail: hassan.khalid@strath.ac.uk

J. E. Bos
TNO Human Factors, P.O. Box 23,
3769 ZG Soesterberg, The Netherlands

1 Introduction

Motion sickness is a group of common nausea syndromes experienced by most travellers, irrespective of their mode of transportation. However, depending on the transport type, it is termed seasickness, coach sickness, car sickness, airsickness, and even space sickness. Vehicle motions play a key role in initiating the feelings of dizziness, bodily warmth, sweating, drowsiness, yawning, changing mouth dryness levels, headache, stomach awareness, nausea and finally emesis (vomiting). Interestingly, the presence of physical motion is not essential, as visually perceived motions like those encountered in the virtual environment are equally capable of producing these undesirable symptoms (in this case, they are usually termed as cinerama sickness, simulator sickness [1], or cybersickness [2]).

Despite its primeval nature, the theoretical and practical understanding of motion sickness causation has still not fully matured, and research continues to improve the knowledge base for this otherwise commonly encountered issue. Like any other scientific discipline with a similar

level of abstraction, research on motion sickness has followed two (fundamentally) different directions. One approach attempts to understand and model the underlying physiological mechanism responsible for the elicitation of sickness symptoms [2–8]. The other school of thought has focused on the development of descriptive statistical models capable of predicting the proportion of the general population likely to suffer sickness symptoms under given (mostly passive) motion environments [9–17].

Although Alexander et al. [10–13] carried out a number of laboratory experiments however, those of O'Hanlon and McCauley [16] and McCauley et al. [17] were the first systematic endeavors to establish the roles of the amplitude and the frequency of purely (sinusoidal) vertical motion in the occurrence of motion sickness. They exposed over 500 young college male students to vertical sinusoidal motions using 25 combinations of ten frequencies (from 0.083 to 0.7 Hz) and various (RMS) magnitudes (from 0.27 to 5.5 m/s^2). They were able to define mathematical models capable of predicting the proportion of people who would vomit (termed "motion sickness incidence," MSI) under purely sinusoidal vertical motion of known magnitude (acceleration) and frequency.

Later on, Lawther and Griffin [18] carried out field trials aboard six monohull vessels, two hovercraft, and one hydrofoil vessel operating around the British Isles. They recorded almost 300 h of six-degrees-of-freedom vessel motions during 114 voyages ranging from half an hour to 6 h in duration. By integrating the laboratory experimental studies undertaken at Wesleyan University [10–13], Human Factors Research Inc. [16, 17], and their own field trials, they proposed yet another descriptive approach for the prediction of vomiting incidence using vertical motions of monohull vessels [15]. Their work eventually determined the sole standards (BS 6841:1987 [19] and ISO 2631-1:1997 [20]) used by the marine industry to predict the comfort qualities of vessels regarding seasickness.

The descriptive approach offers many advantages due to its simplicity and its pragmatic character. Yet it does not explain the underlying mechanism responsible for the elicitation of sickness symptoms. As Lawther and Griffin [15] put it: "The mathematical descriptions of the effects of the variables are not intended to reflect the underlying mechanisms that cause motion sickness, but are merely a pragmatic approach to a problem with a clearly defined scope."

At the other end of the spectrum, the most comprehensive theory of motion sickness that relies on the morphology and physiology of human motion sensors is the sensory conflict theory. Although it has been developed and refined over a long period of time, Reason [7] may rightly be considered the reformer of the modern version of this theory. The essence of this theory is summarized by Wertheim [21] as follows: "The labyrinthine receptors provide the brain with information about self motions that is incongruent with the sensations of motion generated by other sensory systems such as visual or proprioceptive (somatic) systems and/or the information does not match with what is expected from previous transaction with the motion environment."

Sensory conflict theory has been very successful at providing physiological explanations of sickness-provoking environments; however, being qualitative in nature, it cannot translate this causation into a quantitative proportion of people who are likely to suffer sickness [14]. Oman [5] tried to address this issue by integrating the physiological aspects of the theory with optimal control engineering. He suggested employing observers to implement functional features of the neural mismatch hypothesis [22] in order to predict the expected sense modalities using recent transactions with the spatial environment. This concept forms the cornerstone of all pragmatic physiological motion sickness models. However, the mathematical description of the human sensory system ascribed by Oman [5] remains unsorted.

Simplifying the large set of possible sensory conflicts professed by sensory conflict theory and building on the heuristic model of Oman [5], Bless and co-workers [4, 23] postulated the SV conflict theory of motion sickness. Effectively, they restated the neural mismatch hypothesis [22] as: "All situations which provoke motion sickness are characterised by a condition in which the 'sensed vertical' (sensed gravity) as determined on the basis of integrated information from the eyes, the vestibular system and the non-vestibular proprioceptors is at variance with the 'subjective vertical' (expected gravity) as predicted on the basis of previous experience" [4].

Verveniotis and Turan [24] developed an SV conflict model involving the vestibular system only, and used it to successfully predict the seasickness observed aboard high-speed craft (a catamaran and a Deep-V monohull) [8]. However, atypically of monohulls, they found that significantly high levels of lateral acceleration were exhibited by these vessels. Also, the findings of a recent EU project, COMPASS [25], in line with the conclusion of Tamura and Arima [26], indicate a greater role of horizontal acceleration in the elicitation of motion sickness aboard contemporary vessels than perceived before.

As such, the mathematical implementations of SV conflict theory [2, 4, 8, 23, 24, 27, 28] are capable of predicting multidimensional (rotational velocities, linear accelerations, and gravities) sensory conflict vectors. However, so far, only the conflict pertaining to the gravity differences (sensed and expected), termed as "SV conflict," has been used to predict motion sickness in passive motion environments. This paper investigates the potential

improvement of existing SV conflict models by explicitly considering the conflict between the sensed and expected horizontal linear accelerations for predicting seasickness. Firstly, the theoretical aspects of the proposed model, termed as the SVH (subjective vertical–horizontal) conflict model, are discussed. Thereafter, the mathematical details of the new model are outlined. The paper concludes by presenting the successful application of the SVH conflict model to seven field trials of three contemporary vessels. Statistical comparisons of the observed MSIs (during the field trials) with the values predicted by the SVH conflict, SV conflict, and ISO [20]/BS [19] sickness prediction models are also given.

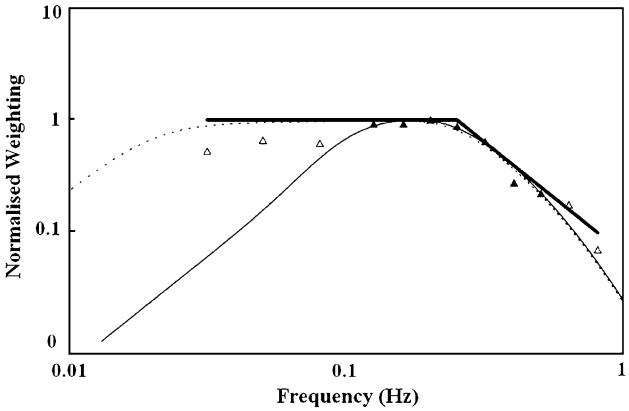

Fig. 1 Comparison of lateral [*solid thick line* (asymptotic); *dotted line* (realizable)] and vertical [*solid thin line*] accelerations frequency weightings (Donohew and Griffin [34])

2 Theoretical premise

The known literature on motion sickness provoked by purely horizontal (fore-and-aft and/or lateral) oscillations is rather limited; there are no studies that parallel the works of O'Hanlon and McCauley [16] and McCauley et al. [17]. Nevertheless, Golding and co-workers [29–33] did conduct a series of laboratory experiments to compare the relative nauseogenity of fore-and-aft sinusoidal oscillations and vertical motions. Golding et al. [32] reported that horizontal motions (fore-and-aft) are twice as nauseogenic as vertical motions in the sitting upright position. In that position, at least double the duration of exposure to vertical oscillations is required to produce sickness levels similar to those produced by horizontal motions of identical frequency and magnitude. Recently, Donohew and Griffin [34] carried out laboratory experiments to study the effects of lateral oscillations on motion sickness. They have proposed frequency weightings, based on the mild nausea, for horizontal accelerations, as shown in Fig. 1. It can be seen from the figure that, in contrast to purely vertical motions, the sickness is independent of oscillation frequency below 0.20 Hz. It may be noted that in certain conditions (shown by open triangles in Fig. 1) the reported incidence of mild nause were not statistically different from static condition, however, the overall sickness level was significantly different.

The findings of the aforementioned studies on purely horizontal motion induced sickness raised the following concerns about existing SV conflict models:

- Being based on the vestibular system only, the SV conflict models of Bos and Bles [23] and later Verveniotis [8] do not distinguish between the sensory conflict resulting from purely vertical and purely horizontal oscillations.
- The SV conflict models postprocess a single conflict (between gravities), so they do not take into account the lower latency exhibited by purely horizontal oscillation induced sickness. Real ship motions involve six degrees of freedom, and this shortcoming may influence the predicted sickness. This would especially be true of contemporary ships with high levels of horizontal acceleration.
- The final point relates to the frequency response of SV conflict models. While simulating the laboratory experiments of McCauley et al. [17], Bos and Bles [23] selected and adjusted the parameters of the internal observer to ensure a peak around 0.2 Hz with a decline in SV conflict on either side of the peak. Though this frequency response is valid for purely vertical motions, it is not suitable for purely horizontal motions below 0.2 Hz, as identified by Donohew and Griffin [34].

One solution to the abovementioned issues, as proposed by Bos et al. [35], would be to independently translate the magnitude and orientation effects of the SV conflict vector into MSIs. The idea is very simple: if the perturbations from the vessel/vehicle motions are solely vertical, then the sensed and expected gravity vectors would remain aligned. In such cases, the orientation difference would be zero, and only the magnitude differences would exist. However, in all other motion combinations both effects (magnitude and orientation) would prevail. Bos et al. [35] assumed that the orientation differences lead to fast effects, such as cross-coupled Coriolis effects [36]. Hence, these differences were accumulated over time using a fast integrator with a time constant of tens of seconds. On the other hand, a slow accumulator with a time constant of several minutes was suggested for the magnitude effects. However, any practical demonstration of this approach by Bos et al. [35] has been limited to combined sway-and-roll motions only, with the predicted sickness being much higher than the expected values.

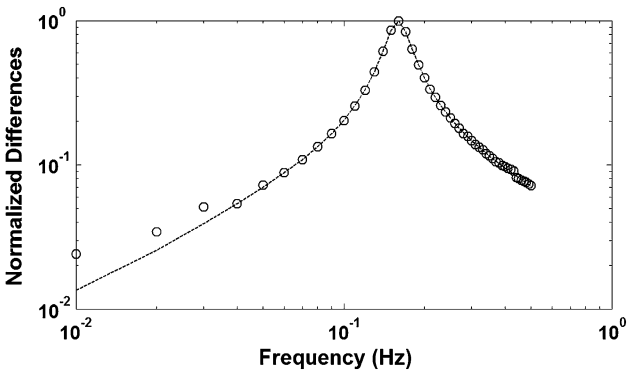

Fig. 2 Normalized orientation (*dotted line*) and magnitude (*circles*) differences of subjective vertical conflict under sinusoidal sway and heave oscillations, respectively

Moreover, the independent processing of orientation and magnitude effects of the SV conflict only addresses the first two anomalies discussed above. In order to re-emphasize this, the normalized orientation and magnitude differences of sensory conflict predicted by the SV conflict model [8] of pure sway and heave oscillations are shown in Fig. 2. In both cases, the simulated sinusoidal oscillations have unit RMS amplitude and frequencies varying from 0.01 to 0.5 Hz.

It can be seen from the above figure that the frequency response of the normalized orientation differences under purely horizontal oscillations (sway) is similar to the frequency behaviour of the magnitude differences under purely vertical (heave) motions. Thus, the output (MSI) frequency response of the SV conflict model for purely horizontal motions would be identical to its response under purely vertical oscillations. Consequently, splitting the SV conflict into magnitude and orientation effects may not work well when attempting to predict sickness under purely horizontal oscillations and in combinations with motions characterized by other degrees of freedom.

In this work we identify another sensory conflict that is readily predictable by SV conflict theory, between the sensed and expected horizontal accelerations, which we shall refer to as the *subjective horizontal (SH) conflict*. These accelerations are respectively defined as the components of gravito-inertial acceleration normal to the sensed and subjective verticals. We postulate that combining SH conflict with SV conflict may improve the ability of SV conflict theory to predict motion sickness. We rephrase the theory as follows: "Any situation that produces a variance between the vertical (gravity) sensed through human sense modalities and the subjective vertical expected (by the nervous system) from past exposure to the spatial environment causes motion sickness. In addition, any difference between the horizontal acceleration (normal to gravity) sensed through the integrated sensory system and that expected from previous experience (i.e., subjective horizontal acceleration) also elicits motion sickness."

We refer to the new model, driven by the above statement of SV conflict theory, as the *subjective vertical–horizontal (SVH) conflict model*. In this work, we limit the human motion-sensing modalities we consider to the vestibular apparatus only, which is also indispensable for motion sickness etiology and has well-defined mathematical models. Thus, the SVH conflict model is identical to any SV conflict model [2, 4, 8, 23, 24, 27, 28], but with the following enhancements:

- Addition of a simple vectorial process to estimate the sensed horizontal acceleration as the component of gravito-inertial acceleration normal to the sensed vertical
- Creation of a process identical to that described above in the internal model to estimate the expected (i.e., subjective) horizontal acceleration.
- Calculation of subjective horizontal (SH) conflict as the vector difference between the sensed and subjective horizontal accelerations.
- Addition of a relatively fast (twice as fast as the SV conflict) integrating path for the postprocessing of the SH conflict into MSI

The overall MSI for a given motion environment would then be a simple combination of the sickness proportions attributable to SV and SH conflicts. It is important to note that in the SVH conflict model, most of the motion sickness elicitation variability is explained by the SV conflict (the rest is estimated using the SH conflict).

3 SVH conflict model

The functional block diagram of the SVH conflict model is depicted in Fig. 3, which is an extended version of the SV conflict model developed by Verveniotis [8, 24, 27].

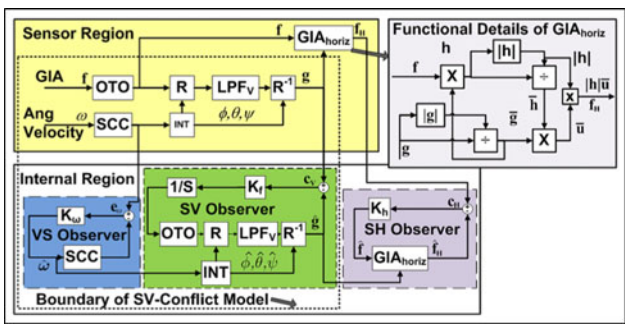

Fig. 3 Schematic diagram of the subjective vertical–horizontal (SVH) conflict model for motion sickness (see text for further information about each block)

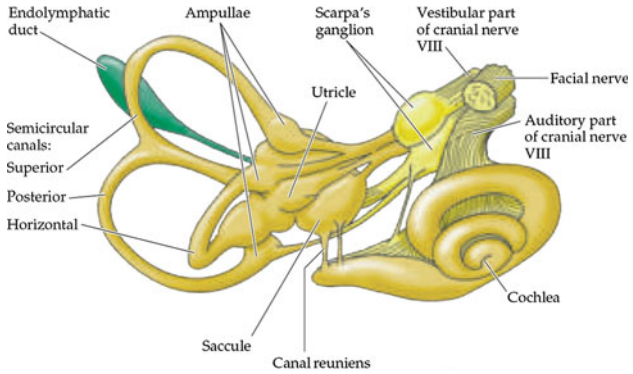

Fig. 4 The labyrinth and its innervations (from [37])

The SVH conflict model is laid out to simulate the vestibular system, which forms one of the special proprioceptive afferent senses and functions of the human inertial guidance system [37]. The labyrinthine receptor organ detects the movement and orientation of its container (the head) in space. It is composed of three bilateral (approximately) orthogonal semicircular canals (superior, posterior, and horizontal), and two otolith systems (the utricles and saccules), as shown in Fig. 4.

Functionally, the canals detect angular acceleration (rotation of the head) and behave like mechanical integrators to estimate the head's rotational velocity. Otoliths, on the other hand, sense and quantify linear accelerations (steady tilt and translational motions). For further details on the morphology and physiology of the vestibular system, see Highstein et al. [38].

The SVH conflict model is based on Luenberger observer theory [39], and comprises two similar but distinctive regions, as depicted in Fig. 3. The sensor region simulates labyrinthine receptors (canals and otoliths) and the physical laws that are assumed to be implemented by the vestibular nuclei to extract information about self-orientation and motions. On the other hand, the internal region—presumably located somewhere in the medulla—is responsible for determining expected orientations and motions. It is assumed that the CNS carries imprints of all human sensory systems and (being aware of their functioning) is able to predict their typical outputs. Thus, variances (that are sufficiently large and long in duration) between the sensed and expected outputs of vestibular system alert the CNS to a possible hallucination (usually caused by toxins). The natural consequence of this is the initiation of nauseogenic malaise [40].

3.1 Estimation of the vertical in the sensor region

Due to their anatomical features, the otoliths act like linear accelerometers, so the equivalence principle [41] prevails and otoliths on their own are unable to distinguish between the tilt (gravitational, $g \times \sin\theta$) and translational accelerations. It is, therefore, imperative to establish information about the self-rotation. This functionality is provided by the semicircular canals. The question that needs to be addressed is how vestibular nuclei distinguish gravity from gravito-inertial acceleration (GIA) registered by the vestibular system. The answer to this question was first provided by Mayne [42] for 2D motions. He suggested low-pass filtering the GIA to separate the (constant) gravity from it.

Thus, the sensor region of the SVH conflict model is laid out to estimate the magnitude and direction of gravity using Mayne's principle generalized to 3D motions [2, 43, 44]. Since gravity is only constant in an Earth-fixed frame of reference, the human head-referenced GIAs (sensed by the otoliths) are first transformed into an Earth-fixed frame of reference using the rotational transformation matrix (R-block of Fig. 3) given by

$$R = \begin{pmatrix} \cos\psi\cos\theta & \cos\psi\sin\theta\sin\phi - \sin\psi\cos\phi & \cos\psi\sin\theta\cos\phi + \sin\psi\sin\phi \\ \sin\psi\cos\theta & \sin\psi\sin\theta\sin\phi + \cos\psi\cos\phi & \sin\psi\sin\theta\cos\phi - \cos\psi\sin\phi \\ -\sin\theta & \cos\theta\sin\phi & \cos\theta\cos\phi \end{pmatrix}, \tag{1}$$

where φ, θ, and ψ are the Euler angles (roll, pitch and yaw) that describe the rotation of a body about a local (i.e., body/head-fixed) frame of reference. The rotation matrix R can be obtained from the signals of semicircular canals (SCC block). After being rotated, the Earth-referenced GIAs are low-pass filtered ($\mathrm{LPF_V}$ block) and transformed back to the head frame of reference (R^{-1} block) using the inverse ($R^{-1} = R^{\mathrm{T}}$) of the rotational matrix given by Eq. 1. A detailed mathematical description of this process is very well covered by Bos and Bles [2, 28] and Turan et al. [27]. Equation 2 represents this complete process of estimating gravity from the GIA:

$$\dot{\mathbf{g}} = \left(\frac{\mathbf{f} - \mathbf{g}}{\tau}\right) - \boldsymbol{\omega} \times \mathbf{g}. \tag{2}$$

Here, $\mathbf{f}$ and $\mathbf{g}$ are the sensed GIA and gravity vectors (boldface letters denote vectors) in the body (head) frame of reference (see Fig. 2 in [27]), $\boldsymbol{\omega}$ is the angular velocity vector as sensed by the canals, and τ is the time constant of the low-pass filter. It can be easily inferred from Eq. 2 that an explicit calculation of the rotational matrices (Eq. 1) is not needed. The angular velocity vector sensed by the semicircular canals would be able to directly account for the rotational effects (for further details, see for example [2]). Based on human sled and centrifuge experiments, Bos and Bles [23] suggest a value of 5 s for τ.

As mentioned earlier, the semicircular canals act like mechanical integrators and have a frequency response similar to a band-pass filter [45]. However, laboratory experiments by O'Hanlon and McCauley [16], McCauley

et al. [17], and Donohew and Griffin [34] suggest a rapid decline in (motion sickness) sensitivity above 0.2 Hz. Moreover, the peak frequencies of typical rigid body motions of real vessels lie within the decade 0.1–1.0 Hz [46]. Thus, for the frequencies of interest (i.e., <0.5 Hz), canals may be treated as high-pass filters with the following transfer function suggested by Merfeld et al. [47]:

$$\frac{\alpha_\omega(s)}{\omega(s)} = \frac{5.7s}{5.7s+1}, \tag{3}$$

where α_ω is the canal afferent response and ω is the angular velocity in the Laplace domain (about any one of the three axes). As far as the otoliths are concerned, their afferents (α_{GIA}) faithfully follow the sensed GIA in the frequency range up to 1.0 Hz [47]. The relevant frequency contents of a real vessel's rigid body motions are far below this range, so a transfer function of unity can be used for simplicity without any significant loss of accuracy.

The transfer functions used in our modeling of the vestibular system, including that of the low-pass filter, are summarized below:

$$\begin{aligned}
&\frac{\alpha_{GIA}(s)}{GIA(s)} = \text{oto}(s) = 1\\
&\frac{\alpha_\omega(s)}{\omega(s)} = \text{scc}(s) = \frac{\tau s}{\tau s+1} = \frac{5.7s}{5.7s+1}\\
&\text{LPF}_V(s) = \frac{1}{\tau s+1} = \frac{1}{5s+1}.
\end{aligned} \tag{4}$$

Since we are dealing with six-degrees-of-freedom motions, the transfer functions of otoliths and canals would be:

$$\begin{aligned}
&\frac{\alpha_f(s)}{\mathbf{f}(s)} = \text{OTO}(s) = \begin{pmatrix} \text{oto}(s) & 0 & 0\\ 0 & \text{oto}(s) & 0\\ 0 & 0 & \text{oto}(s)\end{pmatrix}\\
&\frac{\alpha_\omega(s)}{\boldsymbol{\omega}(s)} = \text{SCC}(s) = \begin{pmatrix} scc(s) & 0 & 0\\ 0 & \text{scc}(s) & 0\\ 0 & 0 & \text{scc}(s)\end{pmatrix}.
\end{aligned} \tag{5}$$

3.2 Estimation of the horizontal in the sensor region

We define the sensed horizontal accelerations as the component of the GIA normal to the sensed gravity (in the body frame of reference). The sensed vertical readily carries the effects of (low-frequency) translational accelerations parallel to it. Thus, this definition of sensed horizontal establishes the component of the GIA that is not accounted for by the SV conflict. The process that is assumed to be used by the CNS to estimate the sensed horizontal acceleration is fairly simple and involves a few vector manipulations. The details of this process are included and expanded as the GIA_{horiz} block in Fig. 3.

Firstly, the vector product of the sensed GIA (**f**) with the unit vector in the direction of sensed gravity ($\bar{\mathbf{g}}$; [bold letters with a bar on top represent unit vectors]) yields the vector **h**. This resultant vector has a magnitude equal to the component of the GIA normal to sensed gravity, but it is directed out of the plane containing them:

$$\mathbf{h} = \mathbf{f} \times \bar{\mathbf{g}} = \{|\mathbf{f}| \cdot |1| \cdot \sin(\gamma)\}\bar{\mathbf{n}} = |\mathbf{f}| \cdot \sin(\gamma) \cdot \bar{\mathbf{n}}, \tag{6}$$

where γ is the angle between the sensed GIA (**f**) and gravity (**g**); while $\bar{\mathbf{n}}$ is a unit vector normal to the plane containing them. We can determine the magnitude of the vector of interest (i.e., $|\mathbf{h}|$), but its direction is incorrect. Now, a cross product of the unit vectors in the direction of **g** and **h** leads to another unit vector, $\bar{\mathbf{u}}$, which is normal to the sensed gravity, directed towards the GIA, and located within the plane containing them:

$$\bar{\mathbf{u}} = \bar{\mathbf{g}} \times \bar{\mathbf{h}}. \tag{7}$$

Simple multiplication of the above unit vector with $|\mathbf{h}|$ gives us the vector of interest:

$$\mathbf{f_H} = |\mathbf{h}| \cdot \bar{\mathbf{u}}. \tag{8}$$

3.3 Estimation of the vertical in the internal region

The segment of the internal region responsible for estimating the expected gravity (subjective vertical) comprises two observers: a velocity storage (VS) and a subjective vertical (SV) observer. The former replicates the velocity storage mechanism [48] needed to predict low-frequency rotational oscillations (as canals act like high-pass filters). The afferents predicted by the VS observer are compared with the sensed afferents of canals, and the difference between the two results into an error signal. This error signal is weighted (K_ω) and fed to the internal model of the canals by the compensator, steering the estimates towards the sensed angular velocity (see Fig. 3). In the case of a step input to the canals, the VS observer retains impressions of the canal afferents for a longer period than would otherwise be exhibited by the first-order neurons innervating the canals.

It is important to note that Bos et al. [49] suggested that the velocity storage mechanism is primarily applicable to horizontal canal afferents. However, this should not be an issue in the present context (where it is applied to all three canal afferents), as the rotational motions of real ships rarely have frequencies below the cutoff frequency (0.028 Hz as per Eq. 3) of the canals. Thus, the VS observer is merely there to facilitate the calculation of the internal estimate of the angular velocity, in line with the orientation model of Merfeld et al. [47]. The outputs of the VS observer (i.e., estimated rotational velocities) are fed into the SV observer to calculate the rotational transformation matrices.

The physical laws embedded in the SV observer to estimate the expected gravity $\hat{\mathbf{g}}$ (i.e., the subjective vertical; note that the boldface letters with hats represent internal/subjective vectors) are identical to those employed by vestibular nuclei in the sensor region. The difference between sensed and subjective verticals ($\hat{\mathbf{g}} - \mathbf{g}$) is the SV conflict vector $\mathbf{c_V}$. This conflict is used by the compensator of the SV observer, via a proportional gain (K_f) and an integrator ($1/s$), to steer internal gravity estimates $\hat{\mathbf{g}}$ towards the sensed gravity $\mathbf{g}$. The frequency response of the SV observer depends on the magnitude of the weighting K_f. Bos and Bles [23] suggest a value of 5 (s^{-1}) for K_f. This causes the conflict to reach its maximum around 1.0 rad/s (0.16 Hz), which corresponds to the frequency at which human beings exhibit maximum sensitivity to vertical oscillations from a motion sickness viewpoint.

3.4 Estimation of the horizontal in the internal region

Similar to the SV observer, the processes implemented by the subjective horizontal (SH) observer are exact copies of those carried out in the sensor region: estimates of the subjective horizontal acceleration $\hat{\mathbf{f}}_\mathbf{H}$ are compared with the sensed values $\mathbf{f_H}$, thus giving rise to the subjective horizontal (SH) conflict $\mathbf{c_H}$. This conflict is weighted (K_h) and fed back to the SH observer through a compensator to minimize the difference between the sensed and subjective horizontal accelerations. The magnitude of K_h (= 1) has been estimated by statistically fitting the SVH conflict model to 15 full-scale trials of a high-speed wave-piercing catamaran vessel ($p = 0.134$; $\chi^2 = 21.09$; $dof = 15$).

3.5 Translation of conflicts into the MSI

Once established, the SV and SH conflicts need to be translated into the MSI, which is defined as the proportion of the passengers who are likely to vomit in a given (ship) motion environment. There are two important features of the MSI that should be taken into account while transforming conflicts: nonlinearity and accumulation. Considering the laboratory data of McCauley et al. [17], Bos and Bles [23] proposed rectification of the SV conflict using the Hill function h given by Eq. 9, to account for the nonlinear characteristics of MSI. Here, h will increase exponentially for small conflicts and logarithmically for large values.

$$h = \frac{|\mathbf{c}|^n}{b^n + |\mathbf{c}|^n}. \tag{9}$$

$\mathbf{c}$ is the conflict vector, and b and n are shape parameters of the Hill function h. We know that people (generally) do not get motion sick instantly upon exposure to a provoking environment, and that they do recover from it upon the removal/reduction of the motions that cause the sickness.

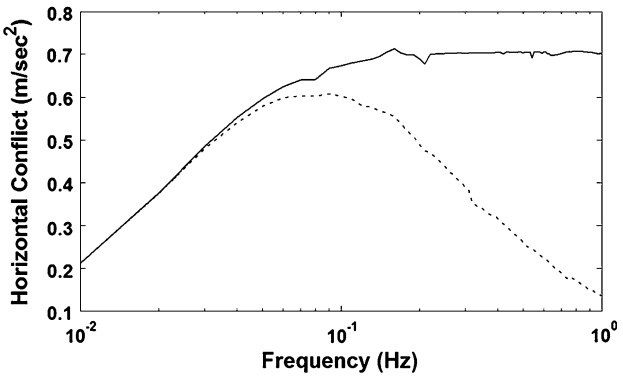

Fig. 5 Frequency response of the SH conflict before (*solid line*) and after (*dotted line*) low-pass filtering

Furthermore, the MSI can only attain a maximum value of 100%; it does not rise infinitely. The mathematical function that can take these accumulation features into account is a second-order low-pass filter termed a "leaky integrator" [23]. Thus, the MSI% can be linked to the rectified SV conflict (i.e., h) by

$$\mathrm{MSI}\% = \frac{K_{\mathrm{MSI}}}{(\mu s + 1)^2} \cdot h. \tag{10}$$

K_{MSI} is the maximum value of the output (i.e., the maximum proportion of the people becoming motion sick) and μ is the filter's time constant. As mentioned earlier, all laboratory experiments concerning the elicitation of motion sickness due to purely horizontal oscillations [33, 34, 50] suggest a decrease in sickness sensitivity to such motions of frequencies >0.2 Hz. In the present arrangement (Fig. 3), the frequency response of the SH conflict is like a high-pass filter (see Fig. 5), which should be adjusted before being translated into the MSI. This is achieved by filtering the conflict using a single-pole low-pass filter with a corner frequency of 0.2 Hz (1.26 rad/s), as given by

$$\mathrm{LPF}_H(s) = \frac{1.26}{s + 1.26} = \frac{1}{0.79s + 1}. \tag{11}$$

The pre- and postfiltered magnitudes of the SH conflicts for purely lateral (sway) motions (unit RMS acceleration) of various frequencies are depicted in Fig. 5. The low-pass filtering of horizontal accelerations suggested here is primarily meant to simulate the subjective sickness sensitivity to purely horizontal oscillations.

The parameters of the conflict rectifier (Eq. 9) and its accumulator (Eq. 10) for the postprocessing of the SV conflict are based on laboratory results for vertical oscillations [17]. However, in the absence of such an abundance of data for horizontal oscillations, we assume that these relationships also exist between the SH conflict and MSI under purely horizontal oscillations. Thus, we estimate the MSI for each conflict (i.e., SV and SH) separately and then

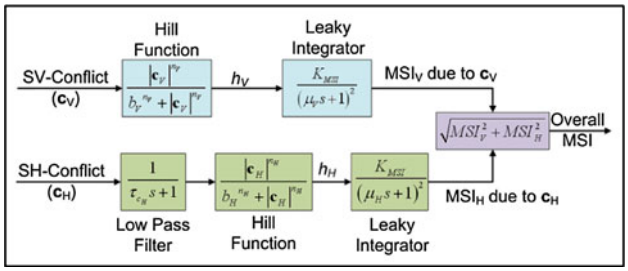

Fig. 6 Schematic diagram of the "emetic brain" part of subjective vertical–horizontal (SVH) conflict motion sickness model

Table 1 Hill function and leaky integrator parameters

Parameter	SV conflict	SH conflict
b	0.7	2.5
n	2	1.0
K_{MSI}	85(%)	85(%)
μ	12 min	6 min

combine them to calculate the overall MSI. It is intuitive that the shape parameters of the Hill function and the time constant of the leaky integrator would be different for the two—fundamentally different—conflicts, as depicted in Fig. 6.

It is not known exactly how the CNS combines the sickness effects of SV and SH conflicts. Therefore, among numerous possibilities, we considered two: simple linear addition, and Pythagoras addition, by treating the $\mathrm{MSI_V}$ (due to SV conflict) and the $\mathrm{MSI_H}$ (due to SH conflict) as sides of a right-angled triangle. Statistical fitting of the SVH conflict model to the 15 full-scale trials of a high-speed wave piercer (used to calibrate the SVH model), revealed that Pythagoras approach ($\chi^2 = 21.09$, $p = 0.134$) is more promising than simple addition ($\chi^2 = 22.73$, $p = 0.090$). Furthermore, the parameters of the Hill function (Eq. 9) and the leaky integrator (Eq. 10) given in Table 1 were found to be optimal.

The parameter values for the postprocessing of SV conflict are exactly the same as those proposed by Bos and Bles [23] to replicate laboratory experiments by McCauley et al. [17]. This preserves the model's capacity to mimic laboratory results for purely vertical oscillations. The time constant of the leaky integrator used to process the SH conflict is set to half the value used for the SV conflict. This is done to account for the lower (by almost half) latency of motion sickness for purely horizontal oscillations [32].

4 Calculation of frequency weightings

We implemented the SVH conflict model in SIMULINK® (companion software to MATLAB® by MathWorks™).

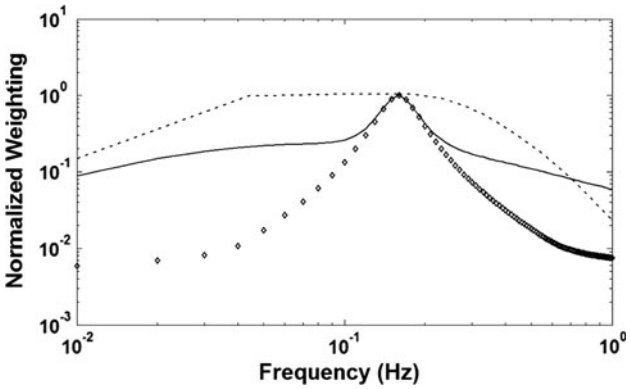

Fig. 7 Normalized frequency weighting for purely horizontal oscillations (unit-RMS accelerations); the SVH conflict model (*solid line*); and the SV conflict model (*diamonds*); Donohew and Griffin [34] (*dotted line*)

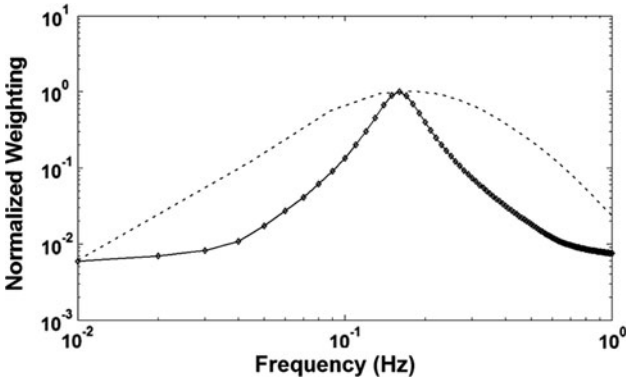

Fig. 8 Normalized frequency weighting for purely vertical oscillations (unit-RMS acceleration); SVH conflict model (*solid line*); SV conflict model (*diamonds*); Lawther and Griffin [18] (*dotted line*)

By running the model for unit-RMS lateral (sway) accelerations and a range of frequencies (0.01–1.0 Hz), we were able to estimate the normalized MSIs caused by the purely horizontal oscillations. When we further normalized these MSIs such that the maximum value was 1.0, the resulting graph—as shown in Fig. 7—represents frequency weightings for purely horizontal motions. This figure also presents normalized frequency weightings calculated using the SV conflict model and those suggested by Donohew and Griffin [34]. The frequency weightings predicted by the SVH conflict model and those obtained through laboratory experiments show similar trends, whereas the SV conflict model suggests that there is a reduction in sickness below and above 0.16 Hz, substantiating the reservations we expressed in Sect. 2.

Likewise, we calculated frequency weightings for purely vertical accelerations by running the SVH and SV conflict models for unit-RMS vertical (heave) accelerations with varying frequencies, as shown in Fig. 8. In this case, the SVH and SV conflict models predict identical weightings that are displaying features similar to the frequency

Table 2 Approximate principal characteristics of the vessels

Ship	Hull form	LBP (m)	Beam (m)	Draught (m)	Speed (knots)	Passengers	Cars	Journey time (h)	Trips
A	MH	160	29	7	20	2500	400	10.0–16.0	3
B	Cat	37	10	2	38	380	Nil	1.5–1.75	1
C	WP	90	25	3.5	40	850	200	3.0–3.8	3

MH monohull, *Cat* catamaran, *WP* wave piercer

weightings derived by Lawther and Griffin [15] for purely vertical oscillations.

We can see that the SVH conflict model, unlike the SV conflict model, presents different frequency responses for purely horizontal and vertical oscillations. It is therefore expected to perform better when large horizontal motions are exhibited by any vessel, and would be similar to SV conflict in other situation.

5 Application to field trails

This section briefly presents the seven field trials of three passenger ferries used to validate the SVH conflict model. Due to commercial sensitivities, the hull forms of the vessels are not reproduced here, but their approximate principal characteristics are summarized in Table 2. The table also indicates the typical journey time and number of field trials of each vessel.

Passenger areas onboard these vessels were divided into various zones to account for the lever-arm effects of the vessels' rotational motions.

5.1 Field measurements

The motion histories of the three vessels were measured and recorded using a motion reference unit (MRU), which consists of three orthogonal linear accelerometers and angular rate Coriolis gyroscopes. The hardware and software of the MRU isolate the parasitic gravity components from the measured gravito-inertial accelerations; thus, the logged accelerations are purely inertial. In addition to recording vessel motions, a survey questionnaire similar to the one used by Turan et al. [27] was distributed amongst the passengers to establish the incidence of motion sickness. A total of 871 responses were collected onboard monohull A, 93 replies were collated aboard catamaran B, and 180 questionnaires were returned by the passengers aboard wave-piercer C.

5.2 Estimation of MSI

In this study, the two physiological motion sickness models (i.e., SVH conflict and SV conflict) were implemented in SIMULINK®. We assumed that the passengers were seated and passively moving with the ship, and that they did not execute any volitional head movements. Thus, we treated the linear accelerations and rotational velocities recorded by the MRU and recalculated for the passenger zones, as a direct input to the labyrinthine apparatus. In return, the models estimated the proportion of people likely to vomit in each zone. Since the distribution of passengers among the various zones varies (very few people stick to one place throughout the journey), and we do not have information on their exact dispersal throughout each journey, we assumed that they were equally distributed in all zones. Thus, the MSI averaged across all considered passenger zones represents the overall MSI for a particular trip of a given vessel.

As far as the descriptive model (ISO 2631-1:1997/BS 6841:187) is concerned, we implemented the time-domain version of it described in the standard.

5.3 Statistical evaluation

The factors listed in Table 3 are known to influence the susceptibility (inclination) of a person to become seasick [3, 14, 18, 51, 52]. Since the real passenger population is likely to exhibit significant variations in these features, we treated the seasickness response of the population as a random variable.

Also, MSI is a dichotomous variable at the individual level (a person may or may not vomit). So, under the assumption of independence (of the individual emesis event), the MSI may be represented by a discrete binomial distribution. If the hypothetical (model) estimate of the proportion of passengers that can get seasick is p_{VI}, the likelihood (p value) of observing n vomiting incidences during the field trial of a vessel where N passengers return the questionnaire is given by:

$$p = \sum_{k=0}^{N} B(k,N,p_{\mathrm{VI}}) \quad \forall\, B(k,N,p_{\mathrm{VI}}) \le B(n,N,p_{\mathrm{VI}})$$
$$\text{where,} \quad B(k,N,p_{\mathrm{VI}}) = \frac{p_{\mathrm{VI}}^{k}(1-p_{\mathrm{VI}})^{(N-k)}N!}{k!(N-k)!}. \tag{12}$$

It is important to note that Eq. 12 represents the exact binomial test for small proportions [53] (the null

Table 3 Factors that influence susceptibility to seasickness

Factor	Remarks
Gender	Females have higher susceptibility
Age	There are peaks at around 11 years old in females and 21 years old in males
Past history	People with past experience of motion sickness on other modes of transportation have a higher inclination to get seasick
Sleep deprivation	Lack of sleep exacerbates susceptibility
Psychological features	Introverts tend to exhibit greater motion sickness
Activity	Tasks requiring mental concentration reduce susceptibility
Temporal aspects	Consumption of alcohol, inflammation of the inner ear, headaches and gastrointestinal disorders make a person more susceptible

Table 4 Observed and predicted MSIs

Trip	Observed			ISO/BS		SV		SVH	
	N	VI	MSI (%)	MSI (%)	*p*	MSI (%)	*p*	MSI (%)	*p*
Vessel A									
1	262	4	1.53	4.84	0.009	1.05	0.359	1.59	1.000
2	388	8	2.06	5.51	0.002	2.66	0.634	2.95	0.368
3	221	4	1.81	5.77	0.008	2.74	0.536	3.01	0.427
Vessel B									
1	93	6	6.45	5.54	0.648	7.08	1.000	7.79	0.846
Vessel C									
1	67	0	0.00	3.63	0.180	1.37	1.000	2.38	0.413
2	76	2	2.63	4.27	0.774	1.20	0.231	2.11	0.676
3	37	1	2.70	2.98	1.000	1.12	0.340	2.09	0.542

N total replies, *VI* people reported to have vomited

hypothesis H_0 is that the observed MSI is not different from model estimates). Hence, at the 5% significance level, the larger the magnitude of p, the better the statistical fitness of the considered model for the relevant field trial. However, in the case of multiple (N_{trials}) trials, it is necessary to establish the overall fitness of each model (SVH, SV and ISO/BS). This can be achieved using the chi-square goodness-of-fit test, where the chi statistic can be calculated using [54]

$$\chi^2 = \sum_{i=1}^{N_{trials}} -2\ln(p_i). \tag{13}$$

Here p_i is the likelihood value calculated using Eq. 12 for the ith field trial. Since, p_i is a normally distributed random variable, by definition, Eq. 13 will yield chi statistics that can be used to estimate the one-tailed probability of a chi distribution with N_{trials} degrees of freedom. This probability represents the overall fitness p value of all trials and vessels for the model under consideration. Assuming that $p < 0.05$ is significant, we can establish the goodness-of-fit of a given model for multiple field trials of all vessels (larger overall p values indicate better overall model fitness).

6 Results and discussion

The observed and predicted MSIs of individual field trials of the three vessels are given in Table 4, which also contains the exact binomial test p values calculated using Eq. 12. The following can be observed from the table:

Table 5 Overall fitnesses of the motion sickness models in relation to seven trials of three ships

Model	DoF	χ^2	Overall p value
ISO/BS	7	36.864	4.97×10^{-6}
SV	7	9.297	0.2320
SVH	7	7.811	0.3496

- The p values of the two physiological (SVH and SV) models for all trials of the three vessels are highly insignificant, implying that these models have very good statistical fitness.
- The exact binomial test p values for the ISO/BS model are insignificant for the three field trials of vessel C and the single trial of vessel B. However, the model is unable to demonstrate statistical fitness for the three field trials of vessel A.
- The inability of the ISO/BS model to fit any field trial of vessel A may be attributed to the long durations of its voyages, which leads to the adaptation of passengers.

The chi-square goodness-of-fit test statistics for the three MSI models (SVH, SV and ISO/BS), calculated using Eq. 13, are summarized in Table 5. The table also presents the overall p values (supporting H_0). The statistical fitnesses of the considered models to multiple field trials clearly indicate that SVH conflict ($p = 0.3496$) is 20% (based on the chi-statistic ratio) better than the SV conflict model ($p = 0.2320$). However, the overall p values of the ISO/BS models are highly significant, indicating a lack of statistical fitness (mainly caused by the long duration field trials of vessel A).

7 Conclusion

This paper presents an alternate statement of SV conflict theory that aims to improve its ability to predict seasickness. A new physiological model (SVH conflict) has been developed that, in addition to the SV conflict, explicitly takes into account horizontal motions by implementing an additional component in the SV model. The paper has also presented the results of applying the SVH, SV, and ISO/BS models to predict the MSIs observed in the seven field trials of three different vessels operating in different areas of Europe.

The overarching fitness tests applied to all field trials of the three ships indicate that the SVH conflict model is statistically 20% better than the existing SV conflict model. These two physiological models are in turn far superior to descriptive motion sickness estimation methods.

References

1. Crampton G (1990) Motion and space sickness. CRC, Boca Raton
2. Bos JE, Bles W, Groen EL (2008) A theory on visually induced motion sickness. Displays 29(2):47–57
3. Benson AJ (1999) Motion sickness. In: Ernsting J, Nicholson A, Rainford D (eds) Aviation medicine. Butterworth & Heinmann, Oxford
4. Bles W, Bos JE, de Graaf B, Groen E, Wertheim AH (1998) Motion sickness: only one provocative conflict? Brain Res Bull 47(5):481–487
5. Oman CM (1982) A heuristic mathematical model for the dynamics of sensory conflict and motion sickness. Acta Otolaryngol Suppl 392:1–44
6. Oman CM (1998) Sensory conflict theory and space sickness: our changing perspective. J Vestibr Res 8(1):51–56
7. Reason JT, Brand JJ (1975) Motion sickness. Academic, New York
8. Verveniotis CS (2004) Prediction of motion sickness on high-speed passenger vessels: a human-oriented approach. Naval Architecture and Marine Engineering, University of Strathclyde, Glasgow
9. Turan O, Sebastiani L,Ganguly A, BOS J, Lewis CH (2005) COMPASS project: new findings regarding effects of ship motions on human comfort and the way forward. In: Int Workshop on Human Factors Impact on Ship Design, Genova, Italy, 6 Oct 2005
10. Alexander SJ, Cotzin M, Hill CJ, Ricciuti EA, Wendt GR (1945) Wesleyan university studies on motion sickness. 1. The effects of variation of time intervals between accelerations upon sickness rates. J Psychol 19:49–62
11. Alexander SJ, Cotzin M, Hill CJ, Ricciuti EA, Wendt GR (1945) Wesleyan university studies on motion sickness. 2. A second approach to the problem of the effects of variation of time intervals between accelerations upon sickness rates. J Psychol 19:63–68
12. Alexander SJ, Cotzin M, Hill CJ, Ricciuti EA, Wendt GR (1945) Wesleyan university studies on motion sickness. 3. The effects of various accelerations upon sickness rates. J Psychol 20:3–8
13. Alexander SJ, Cotzin M, Hill CJ, Ricciuti EA, Wendt GR (1945) Wesleyan university studies on motion sickness. 4. The effects of waves containing two acceleration levels upon motion sickness. J Psychol 20:9–18
14. Griffin MJ (1990) Handbook of human vibration. Academic, London
15. Lawther A, Griffin MJ (1987) Prediction of the incidence of motion sickness from the magnitude, frequency, and duration of vertical oscillation. J Acoust Soc Am 82(3):957–966
16. O'Hanlon JF, McCauley ME (1974) Motion sickness incidence as a function of the frequency and acceleration of vertical sinusoidal motion. Aerosp Med 45:366–369
17. McCauley M, Royal J, Wylie C, O'Hanlon J, Mackie R (1976) Motion sickness incidence: exploratory studies of habituation, pitch and roll, and the refinement of a mathematical model (Technical Report No. 1733-2). Office of Naval Research (Human Factors Research), Arlington, VA
18. Lawther A, Griffin MJ (1986) The motion of a ship at sea and the consequent motion sickness amongst passengers. Ergonomics 29(4):535–552
19. BSI (1987) Guide to measurement and evaluation of human exposure to whole-body mechanical vibration and repeated shock. The British Standards Institution, London, p 30
20. ISO (1997) Mechanical vibration and shock: evaluation of human exposure to whole-body vibration. Part 1: general requirements. International Organisation for Standardization, Geneva
21. Wertheim AH (1998) Working in a moving environment. Ergonomics 41(12):1845–1858
22. Reason JT (1978) Motion sickness adaptation: a neural mismatch model. J R Soc Med 71(11):819–829
23. Bos JE, Bles W (1998) Modelling motion sickness and subjective vertical mismatch detailed for vertical motions. Brain Res Bull 47(5):537–542
24. Verveniotis CS, Turan O (2002) Prediction of motion sickness in high speed craft. In: RINA High-Speed Craft Conf, London, UK, Nov 2002
25. Turan O (2006) A rational approach for reduction of motion sickness and improvement of passenger comfort and safety in sea transportation (COMPASS Project Technical Report). Universities of Glasgow and Strathclyde, Glasgow
26. Tamura Y, Arima M (2006) Measurement and analysis of ship motion of a high-speed passenger craft. In: Proceedings of the Sixteenth International Offshore and Polar Engineering Conference. International Society of Offshore and Polar Engineers (ISOPE), San Francisco
27. Turan O, Verveniotis C, Khalid H (2009) Motion sickness onboard ships—subjective vertical theory and its application to full scale trials. J Mar Sci Technol 14(4):1–8
28. Bos JE, Bles W, Hosman RJAW (2001) Modelling human spatial orientation and motion perception. In: Proc AIAA Modelling and Simulation Tech Conf, 6–9 Aug 2001
29. Golding JF, Finch MI, Stott JRR (1997) Frequency effect of 0.35–1.0 Hz horizontal translational oscillation on motion sickness and the somatogravic illusion. Aviat Space Environ Med 68(5):396–402
30. Golding JF, Kerguelen M (1992) A comparison of the nauseogenic potential of low-frequency vertical versus horizontal linear oscillation. Aviat Space Environ Med 63(6):491–497
31. Golding JF, Markey HM (1996) Effect of frequency of horizontal linear oscillation on motion sickness and somatogravic illusion. Aviat Space Environ Med 67(2):121–126
32. Golding JF, Markey HM, Stott JRR (1995) The effects of motion direction, body axis, and posture on motion sickness induced by low-frequency linear oscillation. Aviat Space Environ Med 66(11):1046–1051

33. Golding JF, Mueller AG, Gresty MA (2001) A motion sickness maximum around the 0.2 Hz frequency range of horizontal translational oscillation. Aviat Space Environ Med 72(3):188–192
34. Donohew BE, Griffin MJ (2004) Motion sickness: effect of the frequency of lateral oscillation. Aviat Space Environ Med 75(8):649–656
35. Bos JE, Bles W, Dallinga R (2002) Prediction of seasickness with more than one degree of freedom. In: Proc Human Factors in Ship Design and Operation Conf, RINA, London, 2–3 Oct 2002
36. Bles W (1998) Coriolis effects and motion sickness modelling. Brain Res Bull 47(5):543–549
37. Purves D, Augustine GJ, Fitzpatrick D, Hall WC, Lamantia A-S, Mcnamara JO, Williams SM (2004) Neuroscience, 3rd edn. Sinauer Associates, Sunderland
38. Highstein MS, Fay RR, Popper NA (2004) Springer handbook of auditory research: the vestibular system. Springer, New York
39. Luenberger D (1971) An introduction to observers. IEEE Trans Automat Contr 16(6):596–602
40. Treisman M (1977) Motion sickness: an evolutionary hypothesis. Science 197(4302):493–495
41. Einstein A (1907) On the relativity principle and the conclusions drawn from it. Jahrb Radioaktivitat Elektronik 4:411–462
42. Mayne R (1974) In: Kornhuber HH (ed) Handbook of sensory physiology. Springer, Berlin
43. Glasauer S (1992) Das zusammenspiel von otolithen und bogengängen im wirkungsgefüge der subjektiven vertikale (Ph.D. thesis). TU München, München
44. Glasauer S, Merfeld DM (1997) Modelling three dimensional vestibular responses during complex motion stimulation. Three-dimensional kinematics of eye, head and limb movements. Harwood, Amsterdam, pp 387–98
45. Rabbitt RD, Damiano ER, Grant JW (2004) Biomechanics of the semicircular canals and otolith organs. In: Highstein MS, Fay RR, Popper NA (eds) Springer handbook of auditory research: the vestibular system. Springer, New York
46. Guignard J, McCauley M (1990) The accelerative stimulus for motion sickness. In: Crampton GH (ed) Motion and space sickness. CRC, Boca Raton, pp 123–152
47. Merfeld DM, Young LR, Oman CM, Shelhamer MJ (1993) A multidimensional model of the effect of gravity on the spatial orientation of the monkey. J Vestib Res 3(2):141–161
48. Raphan T, Cohen B, Matsuo V (1977) A velocity storage mechanism responsible for optokinetic nystagmus (okn), optokinetic after-nystagmus (okan) and vestibular nystagmus. Contr Gaze Brain Stem Neurons 1:37–47
49. Bos JE, Bles W, de Graaf B (2002) Eye movements to yaw, pitch, and roll about vertical and horizontal axes: adaptation and motion sickness. Aviat Space Environ Med 73(5):436–444
50. Griffin MJ, Mills KL (2002) Effect of frequency and direction of horizontal oscillation on motion sickness. Aviat Space Environ Med 73(6):537–543
51. Bos JE, Damala D, Lewis C, Ganguly A, Turan O (2007) Susceptibility to seasickness. Ergonomics 50(6):890–901
52. Guedry FE (1991) Factors influencing susceptibility: individual differences and human factors. In: AGARD (ed) Motion sickness: significance in aerospace operations and prophylaxis (AGARD-LS-175). Advisory Group for Aerospace Research and Development (AGARD), Neuilly-sur-Seine, p 18
53. McDonald J (2008) Handbook of biological statistics. University of Delaware, Newark (see http://udel.edu/∼mcdonald/statexactbin.html)
54. McKenzie E (2008) Personal discussion regarding goodness-of-fit test for field trials on motion sickness. Department of Statistics and Modelling Science, University of Strathclyde, Glasgow